Equilibrium, Kinetic, and Thermodynamic Studies for the Retention of Cesium-137 from Wastewater Using a Low-Cost Sorbent

R. M. Maree[1], M. M. S. Ali, Aly A. Helal and Mostafa M. Hamed

Hot Laboratories and Waste Management Center, Egyptian Atomic Energy Authority, 13759, Cairo, Egypt

ABSTRACT

Herein, sorption of ^{137}Cs onto modified activated carbon (MAC) was carried out implying kinetics and equilibrium studies. The sorption results obeyed a pseudo-1st-order kinetic and were applied to different isotherm models. According to the correlation coefficients, R^2, the Langmuir, Freundlich, and Frumkin isotherm models successfully described the obtained data rather than Temkin isotherm. Based on the R^2, the equilibrium data followed the sequence Langmuir>Freundlich>Frumkin>Temkin isotherm. The negative values of Gibbs free energy revealed that the removal process was feasible and spontaneous. The negative values of enthalpy clarified that the process is an exothermic one, suggesting that retention of ^{137}Cs decreased with raising reaction temperatures. The values of $\Delta H \ll 25$ kJ/mol indicating that the adsorption process of cesium ^{137}Cs ions onto MAC is a physical adsorption process while the positive entropy values demonstrated an increase in randomness among the solid-liquid phase during adsorption. Finally, the sorption results revealed that the MAC is a suitable material for the capture of ^{137}Cs from low-level radioactive waste.

1. INTRODUCTION

Undoubtedly, the cesium-137 radionuclide is one of the important fission products occurring in significant amounts (ca. 5.9% yield from one month ^{235}U fission at 1 MW power level) in rad wastes [1]. Besides, its high radio-toxicity and its long half-life (32y) possess a serious threat to human beings if aqueous reprocessed wastes of U-fission are released into our ecosystem [2]. The treatment of such radioactive wastes was done as an important aspect of recent research. Reprocessing of spent fuel primarily consists of the removal of Cs-137, followed by volume reduction & finally caramel before the ultimate disposal of wastes [3]. ^{137}Cs radiotoxic fission yield in radioactive waste and thus the removal of these waste ions is very important.

This subject attracted many researchers on different materials [4]. Cesium enters into the human body easily causing several diseases such as thyroid cancer via possible radiation in living tissues. There are many techniques for ^{137}Cs retention from rad waste such as evaporation, solvent extraction, co-deposition, membrane filtration, ion exchange, & adsorption [5].

Therefore, the phase-out process is insufficient in the presence of a large number of chemicals and high energy consumption. The calculation of associated costs and disposal problems of ^{137}Cs ion units and their management are considered to be major deficiencies in these processes [6]. Particularly, the application of solvent extraction on an industrial scale is restricted by high costs [7]. The rate of performance of inorganic ion exchangers generally outweighs organic ion exchange and this is due to their thermal stability and ionic quality [8,9].

In the past few years, many ion exchanges have been developed to remove radioactive cesium which implied zeolite, metallic hexacyanoferrate ion exchange resin, and various mixed properties [10]. The cost of developing the cesium removal process deterministically remains from the economic point of view. Moreover, natural clay minerals (zeolite, bentonite, and montmorillonite) and additives developed from waste materials (high kiln foams and fly ash) are used as cost-effective agents to remove ^{137}Cs ions. However, the presence of monoclonal cations, especially sodium and potassium, seriously weakens the process of ^{137}Cs as a

result of their competitive interaction [11]. A few years ago some experiments were carried out to remove ^{137}Cs using activated carbon, but the obtained results didn't reach the requested level, e.g, Caccin et al. studied the activated carbon capacity of the coconut shell as an adsorbent for Cs^{+} species but it was very weak adsorbent (<1 mg g^{-1}) [12]. Arifi et al. utilized an Almond shell for extracting the activated carbon as an adsorbent for cesium ions but its capacity was 12.63 mg.g^{-1} [13]. Vanderheyden et al. investigated the treatment of radioactive cesium from radioactive wastewater by activated carbon and the removal rate was found to be 28% of cesium (capacity was 8.5 µg g^{-1}) of rad waste [14]. Recently, many studies focused on the use of alternative low-cost materials (precursors) like activated carbon from agricultural wastes and wood [15]. Corchorus Olitorius stalks (activated carbon AC) are a renewable and abundant resource in different geographical world regions. AC powder is a towardly adsorbent with a microporous structure and a greater surface area. The porous and heterogeneous structure of AC can be improved via an activation process which has a crucial impact on the adsorption performance. On the other side, to remove ^{137}Cs ions the modified activated carbon is still under extensive study.

The objective of the current investigation is carrying out the fabrication, characterization, and analytical applications of activated carbon. Besides, the performance of the ^{137}Cs is investigated using MAC under different experimental conditions involving contact time, pH, initial concentration, and temperature. In addition, adsorption isotherm models as well as thermodynamic and kinetic parameters are evaluated and discussed.

2. EXPERIMENTAL

2.1. Materials:

All the reagents utilized in this work are of analytical grade and obtained from BDH, England. Radiotracer ^{137}Cs is purchased from the Institute of Radioisotopes Ltd and used. First 1000 mg L^{-1} of the cesium ion solution are prepared as a stock solution from which the desired concentrations of Cs^{+} ions solution were diluted to carry out the experiments.

2.2. Preparation of new Activated Carbon (AC):

Activated carbon is developed through successive steps to collect Corchorus olitorius stalks [16] from the farms located in the village of Al-Sahafa- Mashtoul Al-

Souk-Center – Al-Sharkia Governorate. The stalks are leaved to dry in the sun a week and then cut into small pieces of 0.5 to 2 cm. After that 35 g dried sample in (50 vol.%) H_3PO_4 for 48 h is dipped. The dough is filtered and transported to the stainless-steel reactor (diameter 4 cm and 60 cm long) with 1 cm tight ports on both sides and then, it is thermally treated at 500 °C for 2 h. Activated carbon with hot tap water is washed to remove additional acidity and to achieve the pH of the washing solution pH ≈ 6.0. [16].

2.2.3. Fabrication of the modified activated carbon (MAC):

The chemically activated carbon is developed by dipping a known weight in nitric acid solution and hydrogen peroxide [16]. MAC oxidation is performed using 10 g of AC to boil in 200 ml of 5 M HNO_3 for 3 h. The AC sample is continuously washed with distilled water to remove the additional acidity to obtain the washing solution with pH 6 [16].

Another treatment is also immersing the same sample in 100 ml of 30% H_2O_2 solution by weight at room temperature for 24 h. Then filter and dry the filtrate in the oven for 24 h at 120 °C. Yield% = 27.71% and burn-off = 72.28%, stored in a glass container. The output% MAC and% burn-off can be obtained using the following equations:

$$Yield(\%) = \frac{MAC}{AC} \times 100 \qquad [1]$$

$$Burn-off(\%) = \frac{MAC-AC}{MAC} \times 100 \qquad [2]$$

Where MAC is the modified activated carbon mass(g) & AC is the original carbonaceous sample mass(g). The modified activated carbon preparation was done several times from which the yield is the average value of all the effective experiments.

2.4. Kinetic studies:

The kinetic experiments are performed by agitating 6 mL of ^{137}Cs with mixed initial concentration, C_o (100 mg L^{-1}), each bottle (25 mL) containing 30 mg of MAC, and with the approved radiation component. The bottles are well closed and then shacked until the equilibrium is achieved. The mixture is separated by a centrifuge until the solution is completely free from the suspended MAC particles. Radioactive samples are measured by taking 1.0 mL of fluid solution and analyzing it radiantly.

2.5. Sorption isotherms:

Batch sorption of ^{137}Cs is done at 25±2 °C to obtain isotherms. A series of 25 ml test tubes are used, each test tube is filled with 6 ml of ^{137}Cs at different concentrations (100–500 mg/L) and a known amount of MAC (30 mg) is added into each test tube and agitated for various periods. The adsorbed amount, q_e (mg/g) is calculated by:

$$q_e = (C_0 - C_e)\frac{V}{m} \qquad [3]$$

where C_0, C_e, V & m are the initial & equilibrium concentrations of Cs ions (mg/L), the volume of solutions (l), respectively, and m is the weight of MAC sorbent used (g), respectively.

3. RESULTS AND DISCUSSION

The adsorption behavior of cesium radionuclides is inspected using the batch sorption technique. The adsorption process is analyzed by applying various isotherm & kinetic models to experimental data.

3.2. Sorption experiments:

3.2.1. Impact of pH:

This study elucidates the influence of pH on the adsorption of cesium ions from liquid solutions using the developed MAC, whose experiments are performed in the pH range (1.0-12.0) at the ratio of V/m 200 mLg[-1]. As depicted in Fig. 1, the higher amount adsorbed for ^{137}Cs ions was achieved in alkali conditions which increases significantly as the pH of the solution increases (with a maximum amount adsorbed of 18 mg/g) at pH 12.0 as compared to acidic conditions. The optimal pH of the solution is then selected at 12.0 for all the experiments.

It is assumed that H^{+} occupies the active sites of the modified activated carbon MAC in the acidic case. For this reason, ^{137}Cs ions must encounter a disallowed force at concentrated H^{+} ions during the sorption process. So, when the adsorbent surface is in alkaline conditions, the electrostatic interaction among the adsorbent surface and ^{137}Cs ions will increase. Hence,[137]Cs adsorption is enhanced at high pH [17]. Consequently, the negative charge on the sorbent surface in the alkaline medium increases the adsorption of ^{137}Cs ions. Thus, it can be inferred that high pH alters the chemistry of the adsorbent˒s surface, especially the invariant COOH in MAC into COO[-] [17]. The predominant mechanism of cation behavior can be interpreted in the light of the cation exchange between ^{137}Cs and low acidic functional groups on the MAC surface. As a consequence, the cation exchange among a metal ion M^{n+} (Cs^{+}) & H^{+} in

MAC in a dilute aqueous solution, can be represented as follows:

$$n\overline{H}^+ + M_{aq}^{n+} \leftrightarrow \overline{M}^{n+} + nH_{aq}^+ \qquad [4]$$
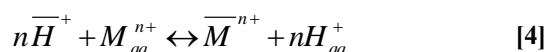
In enough diluted solution, the activity coefficient may be neglected, the equilibrium constant for such reactions is given by:

$$K_H^M = \frac{[\overline{M}^{n+}][H_{aq}^+]^n}{[\overline{H}^+]^n[M_{aq}^{n+}]} \qquad [5]$$

where $[M^{n+}]$ & $[H^+]$ are the concentrations of both metal & hydrogen ions in the solid adsorbent, respectively while $[H^+]$ and $[M^+]$ characterize their concentrations in solution.

3.2.2. Kinetic studies

3.2.2.1. Pseudo-1st-order model:

The pseudo-1st-order model can be evaluated [18] as follows:

$$log(q_e - q_t) = \log(q_e) - \left(\frac{k_1}{2.303}\right)t \qquad [6]$$

where q_e & q_t (mg/g) are the amounts of metal ion sorbed onto MAC at equilibrium and at time t, respectively while k_1 is the pseudo-1st-order rate constant (min^{-1}) which can be estimated from the slope and intercept of the linear plot of $log(q_e - q_t)$ vs. t, as illustrated in Figure 2.

The calculated values of k_1, q_e, & correlation coefficients (R^2) of each plot are given in Table 1. Straight lines obtained from the pseudo-1st-order plots suggest the applicability of this model to fit the experimental data over the initial stage of the sorption process (5–120 min). As depicted in Table 1, the (calculated) q_e values agree well with q_e (experimental). So, the sorption of Cs^{+} ions onto MAC surface is a pseudo-1st-order reaction [19].
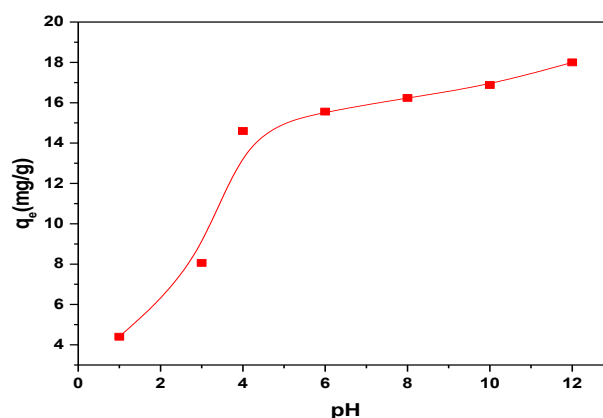

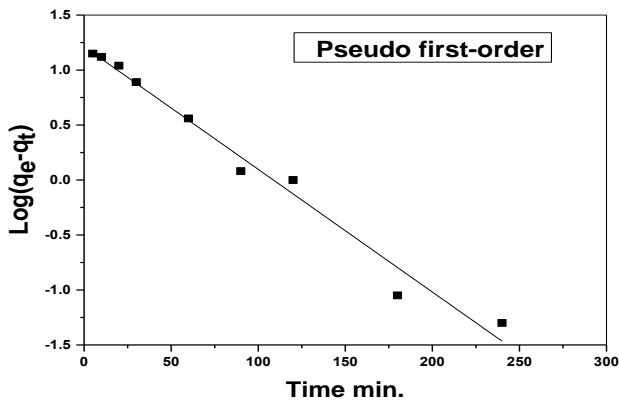**Fig. (1): Effect of pH on sorption of ^{137}Cs by MAC**

Fig. (2): Pseudo first-order plot for the adsorption of ^{137}Cs by MAC

3.2.2.2. pseudo-2nd-order model:

The linearized integral form of the pseudo-2nd-order equation obeys the following Equation [20]:

$$\frac{t}{q_t} = \frac{1}{k_2 q_e^2} + \frac{1}{q_e} t \qquad [7]$$

Where k_2 represents the rate constant of the pseudo-2nd-order equation (g/mg.min). Plotting t/qt against t for Cs$^+$ ions sorption at different temperatures are exhibited in Figure 3.

As cited in Table 1, the values of the initial sorption rate (h) & k_2 raise as the temperature increases. The R^2 extremely approach to unity, and its calculated q_e disagrees with q_e (practical). Hence, the calculated pseudo-2nd-order model cannot be applicable for the sorption of Cs$^+$ ions onto MAC surface. These data prove that the pseudo-1st-order sorption mechanism is predominant and that the overall rate constant of each sorption process appears to be controlled by the physisorption [21].
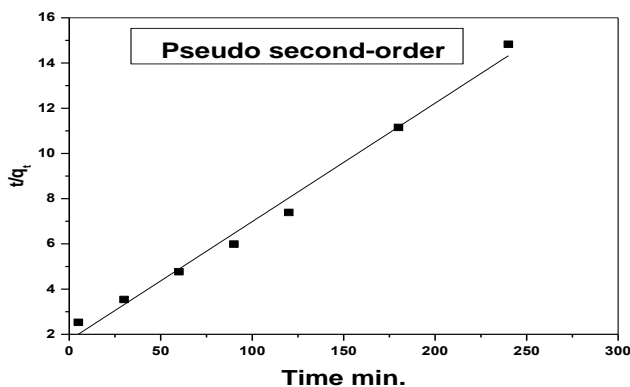

Fig. (3): Pseudo second-order plot for the adsorption of ^{137}Cs by MAC

3.2.3. Sorption isotherms:

The sorption of Cs$^+$ ions onto MAC surface is described via isotherms. The initial rapid sorption slowly approaches the equilibrium at higher concentrations. Several common sorption isotherm models implying Langmuir, Freundlich, Temkin, & Frumkin isotherm models are applied to fit the obtained isotherm results.

3.2.3.1. Langmuir's isotherm:

The Langmuir model assumes that the surface is homogeneous revealing that the adsorption sites have equal sorbate affinity. Also, the adsorption at one site does not affect sorption at the adjacent sites. The formation of monolayer coverage of the adsorbate at the outer surface of the adsorbent is well explained by this model which accounts for the surface coverage by balancing the rate of adsorption and rate of desorption relatively under equilibrium conditions. This model states that the adsorption rate is proportional to the fraction of the open adsorbent surface while desorption rate is proportional to the fraction of the covered adsorbent surface that [22,23]. The linearized relation of the Langmuir equation is given by [24]:

$$\frac{1}{q_e} = \frac{1}{q_{max}} + \frac{1}{b q_{max} C_e} \qquad [8]$$

Where q_{max} & b are a single-layer capacity (mg/g), & Langmuir's constant which is associated with adsorptive energy (L mg^{-1}), respectively. The linear plots of 1/Ce against 1/qe reveal that the sorption of Cs$^+$ ions obeys the Langmuir sorption model. A straight line is obtained with a high correlation coefficient confirming that Langmuir isotherm is applicable for sorption of Cs$^+$ ions onto MAC surface. From the slope and intercept, one can determine the values of sorption equilibrium constant, b, and the monolayer capacity, Q. The features of the Langmuir isotherm can be interpreted by a dimensionless constant, R_L, which is known as the Langmuir separation factor which is estimated by:

$$R_L = \frac{1}{1 + b C_o} \qquad [9]$$

Where R_L values elucidate the adsorption to be unfavorable when $R_L > 1$, linear when $R_L = 1$, favorable when $0 < R_L < 1$, and irreversible when $R_L = 0$.

This implies that the adsorption of Cs$^+$ ions onto MAC surface is a favorable process due to R_L values obtained at all initial concentrations are within the range 0 – 1 which suggests the applicability of this modified carbon MAC adsorbent for Cs$^+$ ions removal [25].

Table (1): Calculated kinetic parameters for pseudo first-order and second-order models for the adsorption of ^{137}Cs

Pseudo-first-order parameter			Pseudo-second-order parameter			$q_{e,exp.}$ (mg/g)
k_1, (min^{-1})	$q_{e,\ calc.}$ (mg/g)	R^2	k_2 (mg g^{-1} min^{-1})	$q_{e,calc.}$ (mg/g)	R^2	
0.026	16.21	0.98	0.57	19.23	0.99	16.23

Table (2): Isotherm parameters for ^{137}Cs adsorption by MAC

Langmuir constants				Freundlish constants		
Q_{max} (mg/g)	R_L	$b(L/m)$	R^2	K_f (mg/g)	n	R^2
28.57	0.1235	0.071	0.996	2.02	1.43	0.990

Temkin constants			Frumkin constants		
K_T (L/mol)	b_T (KJ/mol)	R^2	K (dm^3/mg)	a (mg/g)	R^2
0.692	0.179	0.892	4.94	0.0156	0.91
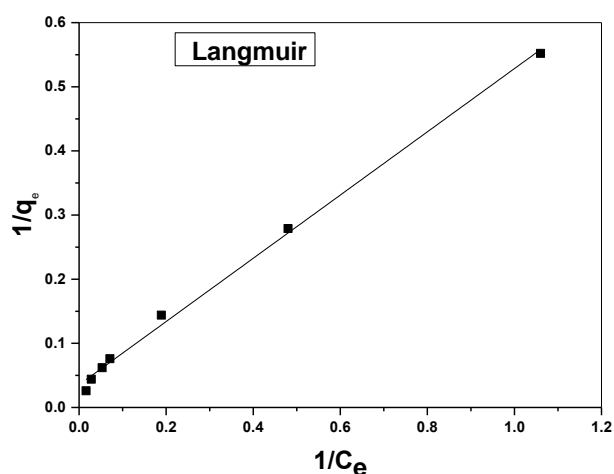
Fig. (4): Langmuir isotherm plot for the adsorption of ^{137}Cs onto MAC
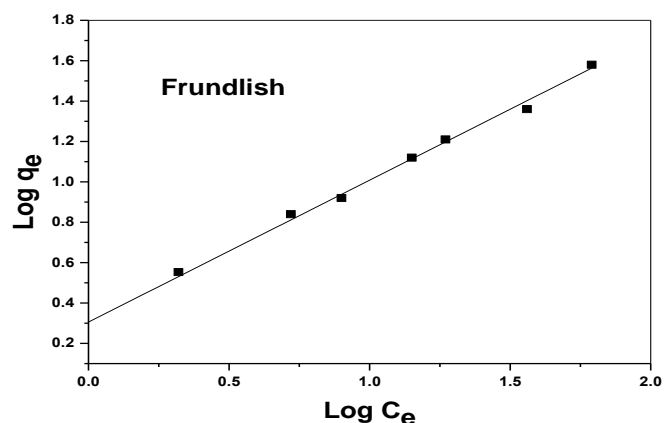
3.2.3.2. Freundlich

The Freundlich adsorption isotherm model refers to the extent of heterogeneity of the adsorbent surface. The adsorptive sites are made up of small heterogeneous adsorption sites each of which is homogeneous [26]. The Freundlich equation may be written as:

$$\log(q_e) = \log(k_f) + \frac{1}{n}\log(C_e) \qquad [10]$$

Where K_f & $1/n$ are constants of the sorption tendency & sorptive capacity, respectively. K_f value reveals the sorption capacity of adsorbent materials, i.e. the greater the K_f value the higher the sorption capacity [27]. The

Plot of log qe vs. log Ce, gives a straight line confirming Freundlich sorption isotherm model, as shown in Figure 5. This means that the theory of multiple layers of adsorptive and adsorbent saturation was responsible for the best suitability provided by the Freundlich model. The applicability of the Freundlich isothermal model to the present data is similar to the sorption studies of ^{137}Cs ions onto the MAC surface. $1/n$ & K_f are determined from the slope & intercept, respectively as cited in Table 2. Since Freundlish's constant n values are higher than unity (indicating the heterogeneity of the MAC surface), it is expected to be a favorable multi-layer adsorption using modified AC [28].

Fig. (5): Freundlich isotherm plot for the adsorption of ^{137}Cs onto MAC

3.2.3.3. Temkin isotherm

Temkin isotherm is the early model describing the adsorption of hydrogen onto platinum electrodes within acidic solutions. The isotherm [29] implies a factor that explicitly takes into account adsorbent–adsorbate interactions. By ignoring the extremely low and large values of concentrations, the model assumes that the heat of adsorption (function of temperature) of all molecules in the layer would decrease linearly rather than logarithmic with coverage [30]. According to Temkin equation, its derivation is characterized by a uniform distribution of binding energies (up to some maximum binding energy) which predicts the gas phase equilibrium (when the organization in a tightly packed structure with identical orientation is not necessary), conversely, complex adsorption systems including the liquid-phase adsorption isotherms are usually not appropriate to be represented [31]. Temkin model is given by [32]:

$$q_e = \frac{RT}{b_T} Ln(k_T) + \frac{RT}{b_T} Ln(C_e) \qquad [11]$$

Where: R, T, k_T, & b_T represent the gas constant (8.314 J.mol^{-1}.K^{-1}), the absolute temperature (K), the equilibrium binding constant corresponding to the maximum binding energy (L.g^{-1}), & the Temkin constant related to the heat of sorption (KJ.mol^{-1}), respectively. The k_T & b_T are obtained from the slope & intercept of a plot of q_e against LnC_e as clarified in Figure 6 and listed in Table 2, respectively. The adsorption data of cesium ions onto the MAC surface revealed physical adsorption because Temkin isotherm constant b was found to be 0.179 KJ mol^{-1}, and this is enhanced by the results of Freundlich modeling. Moreover, R^2 was found to be 0.892 revealing that the data may also obey the adsorption process.
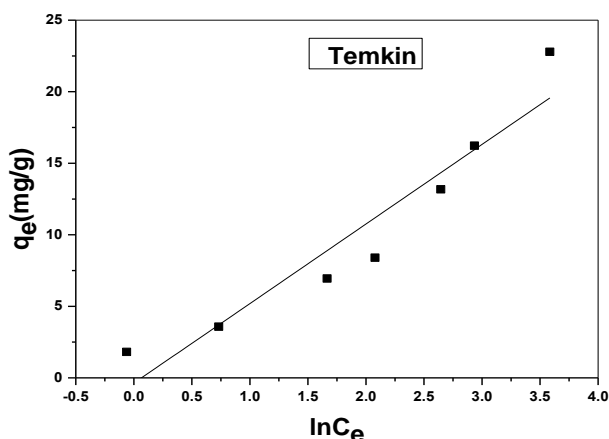

Fig. (6): Temkin isotherm plot for the adsorption of ^{137}Cs onto MAC

3.2.3.4. Frumkin isotherm

The Frumkin isotherm assumes the homogeneous surface of the adsorbent which used a constant term 'a' standing for the interaction of adsorbate molecules with the adsorbed layer. The positive value of 'a' indicated that during adsorption the energy increased due to the lateral interaction of the adsorbate molecule with the adsorbent surface. The negative value of 'a' pointed out that the repulsive force was operated between the incoming adsorbate molecules and the molecules settled on the surface of the adsorbent [33]. The linear form of Frumkin isotherm [34] is given by:

$$\log\left(\frac{Q_e}{1-Q_e}\right) \times \frac{1}{C_e} = \log(k) + 2a \times Q_e \qquad [12]$$

Where K & a are the adsorption-desorption constant and the coefficient of reaction, respectively can be positive or negative. The +Ve value reveals that the adsorption energy increases as the lateral attraction among the adsorbed molecules raises while the -Ve value elucidates that there is a lateral repulsive force among the molecules in the adsorbed layer.

The plot of $\log\left(\frac{Q_e}{1-Q_e}\right) \times \frac{1}{C_e}$ vs Q_e, is a linear relationship as seen in Fig. 3(d). The values of (K)&(a) for adsorption of ^{137}Cs ions onto MAC are evaluated from the intercept and slope, respectively as depicted in Fig. 7 and Table 2, and has a +Ve value of (a= 0.0156 mg/g). The values of K is equal to 4.94 dm^3/mg for ^{137}Cs while the +Ve value of a is 0.0156 mg/g.

The results of ^{137}Cs ions sorption equilibrium by different isotherm models are reported in Fig.3 (a-d). R^2 values are cited in Table 2. An assessment of correlation coefficients of the regarded isotherm models clarified that all the isotherms·s models under the study described the data reliably rather than Temkin isotherm model at the considered concentrations.

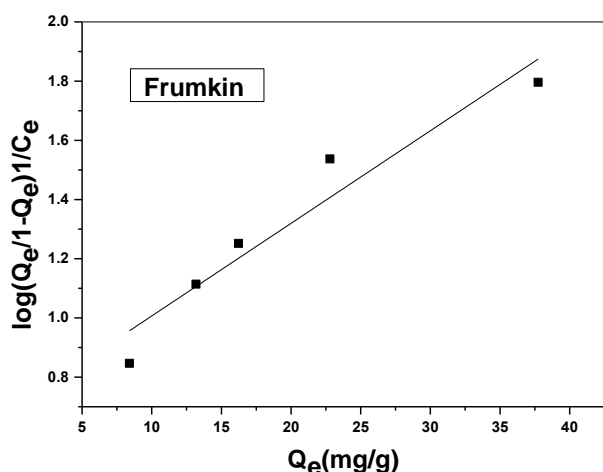Based on the R^2 values, the equilibrium data obey the sequence: Langmuir >Freundlich >Frumkin> Temkin isotherm.

Fig. (7): Frumkin isotherm plot for the adsorption of ^{137}Cs onto *COS-M*.

3.2.4. Thermodynamic studies:

As depicted in Fig. 8, the removal % of ^{137}Cs was plotted against the temperature. The retention % was found to be significantly impacted by temperature change and the marginal minimizes the removal % of ^{137}Cs ions as the temperature raises conducing the heat disturbance by which the movement of ^{137}Cs ions increases and the extension steps commence [35].

The values of enthalpy and entropy changes(ΔH & ΔS), respectively are estimated from the slope and the intercept of the linear plot of ln(K_d) vs. 1/T, as elucidated in Fig. 9 and cited in Table (3).
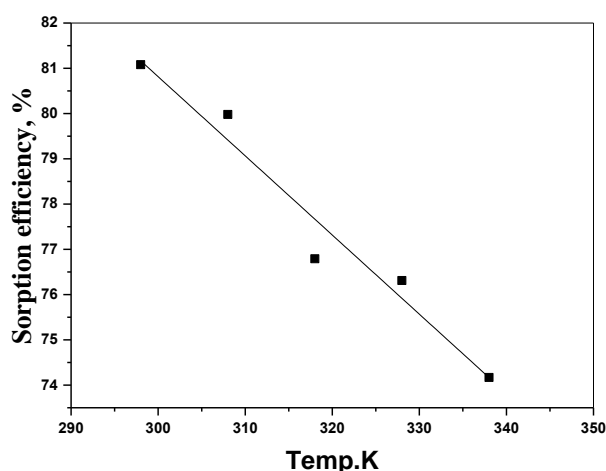

Fig. (8) Effect of temperature on the adsorption efficiency plot for the adsorption of ^{137}Cs by COS-M.
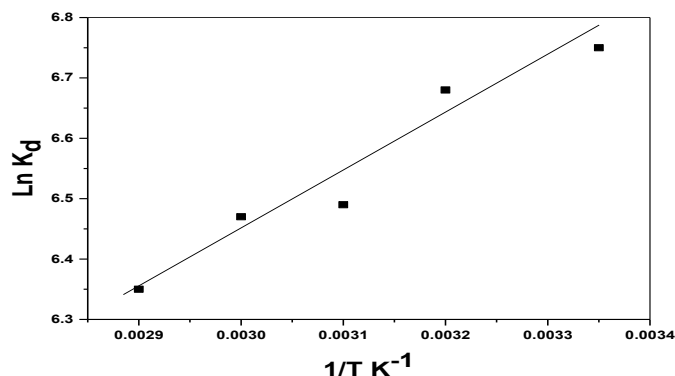

Fig. (9): Van't Hoff plot for the adsorption of ^{137}Cs by COS-M .

Table (3): Thermodynamic parameters for the adsorption of ^{137}Cs on *MAC*

Temp., (K)	R.%	ΔH (KJ/mol)	ΔS (Jmol/K)	ΔG (KJ/mol)
298	81.08			-2.019
308	79.98			-2.056
318	76.79	-0.910	3.72	-2.093
328	76.31			-2.130
338	74.17			-2.168

$$Ln(K_d) = \frac{-\Delta H}{RT} + \frac{\Delta S}{R} \qquad [13]$$

Where K_d (ml g^{-1}) is the distribution coefficient of the ^{137}Cs sorption process. The values of Gibbs free energy change, ΔG, can be evaluated as follows:

$$\Delta G = \Delta H - T\Delta S \qquad [14]$$

The negative ΔG values enhance the feasibility and spontaneous nature of ^{137}Cs sorption onto MAC surface. As the temperature increases, the degree of spontaneity decreases. Positive ΔS values reflect an increased degree of randomness in the solid/liquid surface during the adsorption process of cesium. The thermal expelling nature of Cs$^+$ adsorption onto the modified activated carbon was determined by the negative ΔH values differentiating among the chemical and physical adsorption. The values of ΔH << 25 kJ mol^{-1} reveal that the adsorption process of cesium ^{137}Cs ions onto MAC surface is a physisorption process [36].

3.3. Comparison of adsorption capacity

The adsorption capacity of cesium ions onto MAC-adsorbent was found to be a better adsorbent than the other adsorbent materials as depicted in Table 4.

Table (4): Comparison of ^{137}Cs adsorption by *MAC* with the different activated Carbon based adsorbents

Material	q_{max}(mg/g)	Reference
Walnut shell	4.94	[7]
coconut shell activated carbon	0.76	[12]
Almond shells	12.63	[13]
Pine cone	5.75	[37]
Coal and chitosan	3.00	[38]
Chabazite and activated carbon mix	8.19	[39]
Oxidized multiwall carbon nanotube	12.75	[40]
Bamboo charcoal	0.17	[41]
Graphene oxides	1.46×10^{-3}	[42]
Titanate nanobelt membranes	0.48	[43]
COS-M	**28.57**	**Present work**

CONCLUSIONS

In the current study, we prepared MAC as a low-cost promising material for the removal of ^{137}Cs from radioactive waste. Besides, the obtained data revealed that the overall rate constant of each sorption process that obeyed the pseudo-1st-order is predominant and controlled by the physisorption process. The isothermal adsorption data obey the Langmuir isothermal model. The maximum capacity was found to be 28.57mg.g^{-1}. The ΔG values which are negative enhancing the feasibility and spontaneous nature of ^{137}Cs sorption onto MAC surface. Inspection of the investigated MAC was found to be a higher efficient for removing cesium ions than the other adsorbents in previous studies.

REFERENCES

[1] Khandakera S, Toyohara Y, Kamida S, Kuba T (2018) Adsorptive removal of cesium from aqueous solution using oxidized bamboo charcoal. Water Resour Indust 19: 35-46.

[2] Ashraf MA, Akib S, Maah MJ, Yusoff I, Balkhair KS(2014)Cesium-137:Radio Chemistry, Fate, and Transport, Remediation, and Future Concerns.Critical Reviews in Environmental Science and Technology 44:1740–1793.

[3] Hamed MM, Aly MI, Nayl AA(2016) Kinetics and Thermodynamics Studies of cobalt Strontium and Cesium Sorption on Marble from Aqueous Solution. Chem. Ecol. 32:68-87.

[4] Awual MR, Yaita T, Taguchi T, Shiwaku H, Suzuki S, Okamoto Y(2014)Selective cesium removal from radioactive liquid waste by crown ether immobilized new class conjugate adsorbent. J. Hazard. Mater 278:227–235.

[5] Awual MR, Suzuki S, Taguchi T, Shiwaku H, Okamoto Y, Yaita T(2014)Radioactive cesium removal from nuclear wastewater by novel inorganic and conjugate adsorbents. Chem. Eng. J. 242:127–135.

[6] Pangeni B, Paudyal H, Inoue K, Ohto K, Kawakita H, Alam S(2014)Preparation of natural cation exchanger from persimmon waste and its application for the removal of cesium from water. Chem. Eng. J. 242:109–116.

[7] Ding D, Zhao Y, Yang S, Shi W, Zhang Z, Lei Z, Yang Y (2013) Adsorption of cesium from aqueous solution using agricultural residue - Walnut shell: equilibrium kinetic and thermodynamic modeling studies. Water Res. 47:2563–2571.

[8] Awual MR, Miyazaki Y, Taguchi T, Shiwaku H, Yaita T(2016)Encapsulation of cesium from contaminated water with highly selective facial organic-inorganic mesoporous hybrid adsorbent. Chem. Eng. J. 291:128–137.

[9] Yang H, Yu H, Sun J, Liu J, Xia J, Fang J, Li Y, Qu F, Song A, Wu T(2017)Facile synthesis of mesoporous magnetic AMP polyhydric composites for rapid and highly efficient separation of Cs+ from water. Chem. Eng. J. 317:533–543.

[10] Ibrahim AB, Abass MR, EL-Masry EH, Abou-Mesalam MM (2021) Gamma radiation-induced polymerization of polyacrylic acid-dolomite

composite and applications for removal of cesium, cobalt, and zirconium from aqueous solutions. Applied Radiation and Isotopes 178:109956-109966.

[11] Liu HJ, Xie SB, Xia LS, Tang Q, Kang X, Huang F(2016)Study on the adsorptive property of bentonite for cesium. Environ Earth Sci 75:148-155.

[12] Caccin C, Giacobbo F, Da Ros M, Mariani M (2013) Adsorption of uranium, cesium, and strontium onto coconut shell activated carbon. J Radioanal Nucl Chem 297(1):9–18.

[13] Arifi A, Hanafi HA (2011) Adsorption of cesium, thallium, strontium and cobalt radionuclides using activated carbon. Asian J. Chem. 23:111–115.

[14] Vanderheyden SRH, Van Ammel R, Sobiech-Matura K, Vanreppelen K, Schreurs S, Schroeyers W, Yperman J, Carleer R(2016) Adsorption of cesium on differenttypes of activated carbon. J Radioanal Nucl Chem 310: 301–310.

[15] Jain A, Balasubramanian R, Srinivasan MP(2016)A Hydrothermal conversion of biomass waste to activated carbon with high porosity: A review. Chem. Engin. J. 283:789–805.

[16] Hamed MM, Ali MMS, Helal AA (2020)Influence of sorption parameters on cesium-137 removal using modified activated carbon obtained from corchorus olitorius stalks. Radiochim Acta 108(10): 799-808.

[17] Kim JO, Lee SM, Jeon C (2014)Adsorption characteristics of sericite for cesium ions from an aqueous solution. J Chem Eng Res Des 92(2):368-374.

[18] Sayed MS, Salama TM, Bakr MF, El Dakrory, AM, Maree RM, Ibrahim IA(2016)A comparative study of SDS- and DSS-functionalized graphene as adsorbents for removal of 137Cs ions from low-level radioactive waste. Global Journal of Chemistry 3(1):111–124.

[19] Sayed MS, Salama TM, Bakr MF, El Dakrory, AM, Maree RM, Ibrahim IA(2016)Synthesis of graphene functionalized with (SDS) for removal of [137]Cs(I) and Ce(III) ions from radioactive waste. Journal of International Environmental Application & Science 11(1):110–123.

[20] El-Kamash AM(2008)Evaluation of zeolite A for the sorptive removal of Cs^+ and Sr^{2+} ions from aqueous solutions using batch and fixed-bed column operations. J Hazard Mater 151:432–445.

[21] Zhang H, Zhu M, Du X, Feng S, Miyamoto N, Kano N(2021)Removal of Cesium from Radioactive Waste Liquids Using Geo-materials. Appl Sci 11:8407-8424.

[22] Langmuir, I., (1916)The constitution and fundamental properties of solids and liquids. Part I solids. J. Am Chem. Soc., 38: 2221-2295.

[23] Langmuir, I., (1918) The adsorption of gases on plane surfaces of glass, mica, and platinum. J. Am. Chem. Soc., 40: 1361-1403.

[24] Rizk SE, Hamed MM, Nayl AA(2016) Adsorption Kinetics and Modeling of Gadolinium and Cobalt Ions Sorption by an Ion-Exchange Resin. Part. Sci Technol. 34:716-724.

[25] Holiel M, Hamed MM, Ahmed IM(2016) Sorption behavior of cesium, cobalt and europium radionuclides onto hydroxyl magnesium silicate. Radiochim Acta 104:873–890.

[26] Saruchi, Kumar V(2019)Adsorption Kinetics and Isotherms for the Removal of Rhodamine B Dye and Pb^{+2} Ions from Aqueous Solutions by a Hybrid Ion-Exchanger. Arabian J Chem 12(3): 316-319.

[27] Ali MMS, Sami NM, El-Sayed AA(2020) Removal of Cs^+, $Sr^{2+,}$ and Co^{2+} by activated charcoal modified with Prussian blue nanoparticle (PBNP) from aqueous media: kinetics and equilibrium studies. J Radioanal and Nuc Chem 324:189–201.

[28] Uematsu Y, Ogata F, Saenjum C, Nakamura T, Kawasaki N (2020) Removing Sr(II) and Cs(I) from the Aqueous Phase Using Basil Seed and Elucidating the Adsorption Mechanism. Sustainability 12:2895-2908,

[29] Tempkin M.I., Pyzhev V., (1940)Kinetics of ammonia synthesis on the promoted iron catalyst, Acta Phys. Chim. USSR 12, 327–356.

[30] Aharoni C., Ungarish M., (1977) Kinetics of activated chemisorption. Part 2. Theoretical models, J. Chem. Soc. Faraday Trans. 73, 456–464.

[31] Kim Y., Kim C., Choi I., Rengraj S., Yi J., (2004)Arsenic removal using mesoporous alumina prepared via a templating method, Environ. Sci. Technol. 38,924–931.

[32] Akalin HA, Hicsonmez U, Yilmaz H(2018) Removal of Cesium from Aqueous Solution by Adsorption onto Sivas Yildizeli (Türkiye) Vermiculite: Equilibrium, Kinetic, and Thermodynamic Studies. Jotcsa 5(1):85–116.

[33] Danish M., Ahmad T., Majeed S., Ahmad M., Ziyang L., Pin Z., Shakeel Iqubal S.M., (2018)Use of banana trunk waste as activated carbon in scavenging methylene blue dye: Kinetic, thermodynamic, and isotherm studies. Bio. tech. Re. 3, 127-137.

[34] Menkiti MC, Ejimofor MI, Ezemagu IG, Uddameri V(2016)Turbid-Metric Approach on the Study of Adsorptive Component of Paint Effluent Coagulation Using Snail Shell Extract. Arab J Sci Eng 41:2527–2543.

[35] Hamed MM, Holiel M, Ismail ZH (2016) Removal of ^{134}Cs and $^{152+154}$Eu from liquid radioactive waste using Dowex HCR-S/S, Radiochim Acta 104:399–413.

[36] Hamed MM, Yakout SM, Hassan HS (2013) Solid-phase extraction of nitrate and nitrite anions using naturally and available sorbent. J Radioanal Nucl Chem 295: 697-708.

[37] Ofomaja AE, Pholosi A, Naidoo EB (2013)Kinetics and competitive modeling of cesium biosorption onto chemically modified pine cone powder. Journal of the Taiwan Institute of Chemical Engineers 44: 943–951.

[38] Mizera J, Mizerová G, Machovič V, Borecká L(2007)Sorption of cesium, cobalt and europium on low-rank coal and chitosan. Water Res. 41:620–626.

[39] Song K, Lee H, Moon H, Lee KJ, (1997)Simultaneous removal of the radiotoxic nuclides ^{137}Cs and ^{129}I from aqueous solution. Sep Purif Technol 12:215–227.

[40] Yavari R, Huang YD, Ahmadi SJ(2011) Adsorption of cesium (I) from aqueous solution using oxidized multiwall carbon nanotubes. J Radioanal Nucl Chem 287:393–401.

[41] Khandaker S, Kuba T, Kamida S, Uchikawa Y (2017)Adsorption of cesium from aqueous solution by raw and concentrated nitric acid-modified bamboo charcoal. J Environ Chem Eng 5:1456–1464.

[42] Wang X, Chen Z, Wang X(2015) Graphene oxides for simultaneous highly efficient removal of trace level radionuclides from aqueous solutions. Sci China Chem 58:1766–1773.

[43] 43. Wen T, Zhao Z, Shen C, Li J, Tan X, Zeb A, Wang X, Xu AW (2016) Multifunctional flexible free-standing titanate nanobelt membranes as efficient sorbents for the removal of radioactive 90Sr and 137Cs ions and oils. Sci. Rep. 6:1–10.